Society of Medical Education & Research

2021, Volume 1, Page No: 137-149
ISSN: 3108-4834

Archive of International Journal of Cancer and Allied Science

O-GlcNAcylation of SPOP Controls Colorectal Cancer Development and Ferroptosis through Modulation of β-Catenin Degradation

Mateusz Piotr Kowalczyk[1]*, Tomasz Adam Piotrowski[1], Krzysztof Marek Nowak[1]

[1]Department of Oncology, Medical University of Warsaw, Warsaw, Poland.

***E-mail** ✉ m.kowalczyk.muw@outlook.com

Abstract

Therapeutic strategies for colorectal cancer (CRC) are often limited by recurrence and resistance to drugs. Ferroptosis, a recently characterized form of programmed cell death, represents a promising avenue for CRC treatment. Speckle-type POZ protein (SPOP), a substrate receptor of the E3 ubiquitin ligase complex CRL3, has a crucial biological role, yet its function in CRC therapy and ability to regulate ferroptosis remain largely unexplored. In this study, we demonstrate that SPOP acts as a tumor suppressor in CRC, suppressing tumor cell proliferation and metastasis while enhancing sensitivity to ferroptosis. Transcriptomic analyses indicated that the Wnt signaling pathway might serve as a potential downstream target of SPOP. Further investigations revealed that silencing SPOP led to elevated β-catenin protein levels, whereas clinical data showed an inverse correlation between SPOP expression and β-catenin levels. Mechanistic studies suggest that SPOP facilitates polyubiquitination and subsequent degradation of β-catenin at the K508 residue. Interestingly, O-GlcNAcylation of SPOP decreases its protein stability and diminishes its binding to β-catenin. Additionally, SPOP promotes CRC ferroptosis by suppressing the β-catenin/SLC7A11 axis. Co-treatment with the SPOP-targeting drug maprotiline and a ferroptosis inducer exhibited synergistic antitumor effects in CRC cell lines and xenograft models. Collectively, these results reveal the multifaceted role of SPOP in CRC and suggest that activating SPOP may enhance the efficacy of ferroptosis-based therapies.

Keywords: O-GlcNAcylation, SPOP, β-Catenin, Cancer

Introduction

Colorectal cancer (CRC) is the most prevalent malignancy of the digestive system and ranks among the leading causes of cancer-related mortality [1]. Many patients present with metastatic disease at diagnosis [2], necessitating interventions such as chemotherapy and immunotherapy, yet resistance to these therapies contributes to poor survival outcomes [3]. Aberrant activation of the Wnt signaling pathway occurs in nearly all CRC cases [4], highlighting its critical role in driving disease progression.

Access this article online https://smerpub.com/

Received: 06 February 2021; **Accepted:** 15 May 2021

How to cite this article: Kowalczyk MP, Piotrowski TA, Nowak KM. O-GlcNAcylation of SPOP Controls Colorectal Cancer Development and Ferroptosis through Modulation of β-Catenin Degradation. Arch Int J Cancer Allied Sci. 2021;1:137-49. https://doi.org/10.51847/ZJ2fVmjo1N

Cullin-RING ligases (CRLs) represent the most widely expressed family of E3 ubiquitin ligases in humans [5]. Structurally, CRLs consist of a cullin scaffold, a RING-box protein (RBX1/2), an adaptor, and a substrate receptor. Among them, CRL3, implicated in tumorigenesis, specifically utilizes proteins containing a BTB domain as substrate adaptors [6]. Despite its biological importance, CRL3's precise regulatory mechanisms remain incompletely understood. Speckle-type POZ protein (SPOP) functions as a substrate-binding receptor within CRL3 and can mediate both degradative and non-degradative polyubiquitination of multiple substrates. SPOP's ubiquitination activity relies on its MATH domain, which recognizes the SPOP-binding consensus (SBC) motif, and its BTB domain, which interacts with CUL3 [7, 8]. Previous reports indicate that SPOP acts as a tumor suppressor in various cancers [9–14], including its ability to promote STAT3 degradation and inhibit bladder cancer progression [15].

Notably, SPOP exhibits a high mutation frequency in human tumors, predominantly within the MATH domain, leading to functional inactivation and tumor progression, particularly in prostate and endometrial cancers [16]. However, the role of SPOP in CRC, the dependency of its effects on ubiquitination, and the identification of its specific substrates and pathways remain largely unexplored.

Ferroptosis is an iron-dependent form of programmed cell death driven by disrupted cellular redox balance [17, 18]. It can suppress tumor cell proliferation, invasion, and metastasis and improve responses to radiotherapy and immunotherapy [18, 19], highlighting its potential as a cancer treatment strategy. SLC7A11, a subunit of the cystine/glutamate antiporter Xc–, mediates cystine uptake [20], and the ferroptosis inducer erastin triggers ferroptosis by inhibiting SLC7A11-mediated cystine transport [21]. Overexpression of SLC7A11 is observed in multiple cancers, including CRC [22], and targeting SLC7A11 promotes ferroptosis through lipid peroxidation and iron accumulation, potentially restoring chemotherapy sensitivity [23].

In the present study, we identified CRL3-SPOP as a CRC-associated tumor suppressor that enhances susceptibility to ferroptosis. Mechanistically, SPOP interacts with β-catenin, facilitating its ubiquitination and degradation, which limits β-catenin's ability to activate SLC7A11 transcription. Additionally, SPOP undergoes O-GlcNAcylation mediated by O-GlcNAc transferase (OGT), which decreases SPOP stability and reduces its β-catenin binding, thereby promoting CRC progression. Finally, combination treatment with the SPOP-targeting agent maprotiline and a ferroptosis inducer synergistically inhibited CRC growth, offering a novel therapeutic approach for CRC management.

Results and Discussion

SPOP expression is downregulated in CRC and correlates with better prognosis

We initially compiled a list of 37 CRL3-related genes from the IUUCD database and identified differentially expressed genes (DEGs) in TCGA-COAD and TCGA-READ datasets, which yielded seven overlapping candidate genes **(Figure 1a)**. Prognostic analysis of these candidates highlighted SPOP as a key gene of interest **(Figure 1b)**. Database interrogation revealed that SPOP expression is lower in CRC tissues compared with normal tissues **(Figure 1c)** and that higher SPOP expression correlates with longer survival in CRC patients **(Figure 1d)**. Single-cell analysis using dataset EMTAB8107 showed that SPOP expression is primarily localized in myofibroblasts and relatively low in tumor cell subpopulations **(Figure 1e)**. These findings indicate that SPOP is downregulated in CRC and that its higher expression is associated with improved prognosis.

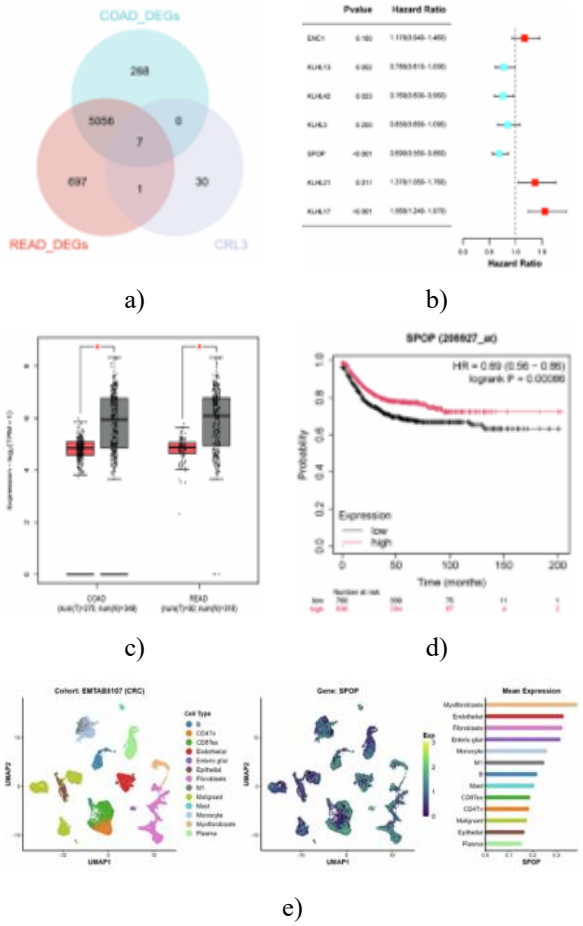

Figure 1. Reduced SPOP Expression in CRC Correlates with Improved Prognosis. **a**The Venn diagram illustrates the overlap between differentially expressed genes (DEGs) identified in the TCGA-COAD and TCGA-READ datasets and CRL3-associated genes. **b** Forest plot presenting candidate genes identified through univariate Cox regression analysis. c SPOP expression levels in COAD and READ tumor samples compared with normal tissues, obtained from GEPIA. d Kaplan–Meier analysis of recurrence-free survival (RFS) in CRC patients stratified by SPOP expression using the Kaplan–Meier Plotter online tool. e t-SNE visualization of

SPOP expression across various subpopulations in human CRC samples via single-cell sequencing.

SPOP suppresses CRC progression

To explore the functional role of SPOP in CRC, we generated SPOP-knockdown cell lines **(Figure 2a)**. CCK8 assays demonstrated that silencing SPOP enhanced CRC cell proliferation **(Figure 2b)**, and cell cycle analysis revealed that SPOP depletion altered the distribution of cell cycle phases **(Figure 2c)**. Additionally, SPOP knockdown promoted cell migration and invasion, as evidenced by wound healing and transwell assays **(Figures 2d–2g)**. Invadopodia formation, a hallmark of metastatic potential characterized by colocalization of F-actin and Cortactin, was markedly increased following SPOP depletion, as shown by immunofluorescence **(Figure 2h)**. Furthermore, in a lung metastasis colonization model, the shSPOP group developed significantly more metastatic nodules **(Figure 2i)**, confirming that SPOP inhibits metastasis. Collectively, these findings indicate that SPOP functions as a tumor suppressor in CRC.

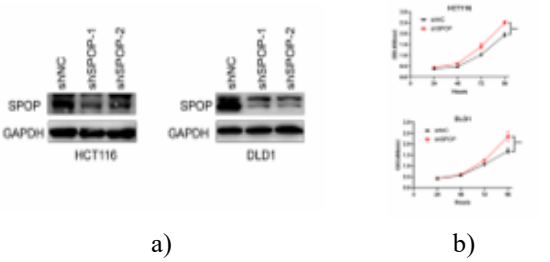

a) b)

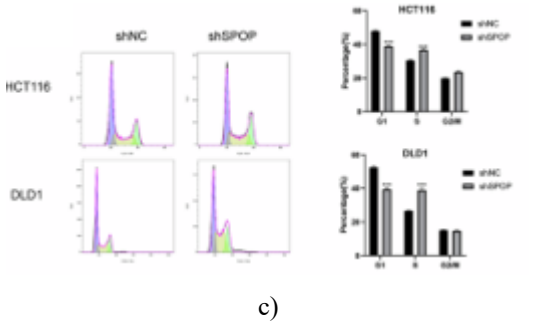

c)

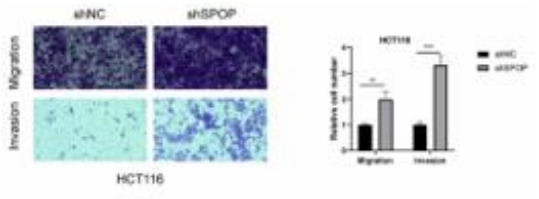

d)

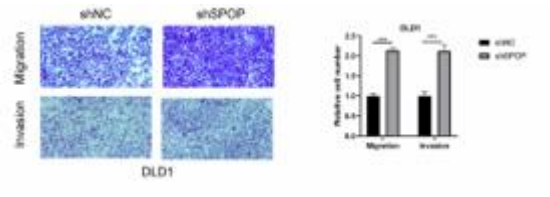

e)

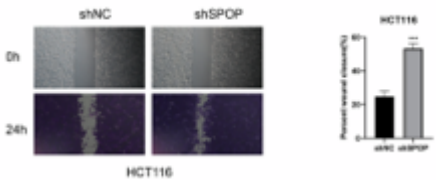

f)

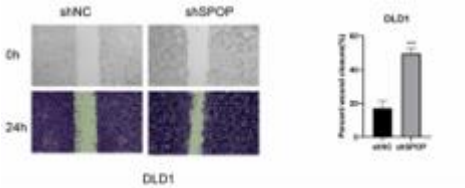

g)

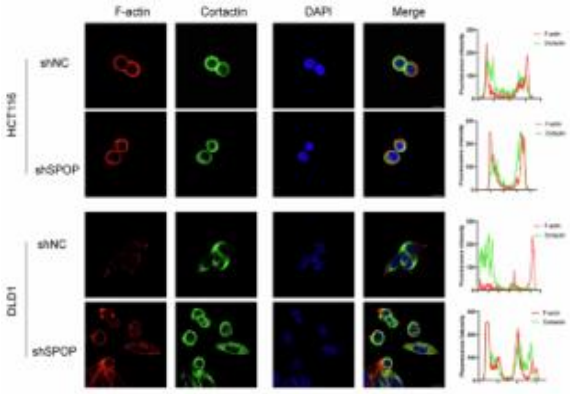

h)

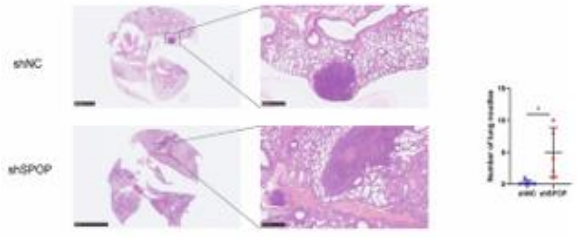

i)

Figure 2. Loss of SPOP accelerates CRC progression **a** HCT116 and DLD1 cells were transduced with lentiviruses carrying SPOP-targeting shRNAs, and knockdown efficiency was confirmed by western blot analysis. **b** CCK-8 assays revealed that silencing

SPOP markedly enhanced the proliferation of CRC cells. **c** Flow cytometry demonstrated that SPOP depletion altered cell cycle distribution, with representative plots and quantitative data shown. **d, e** Transwell assays indicated increased migratory and invasive capacities in SPOP-knockdown cells. **f, g** Wound healing assays further confirmed accelerated cell motility upon SPOP silencing. h Immunofluorescence analysis showed that invadopodia formation, identified by the colocalization of Cortactin and F-actin, was significantly elevated in cells lacking SPOP. i Lung metastasis assays demonstrated that mice injected with shSPOP-expressing HCT116 cells developed more metastatic nodules than controls; representative images and quantification are shown (N = 5, scale bars, 500 μm).

SPOP directly associates with β-catenin

To clarify how SPOP exerts its tumor-suppressive effects in CRC, RNA sequencing was performed on HCT116 cells overexpressing SPOP **(Figure 3a)**. Gene set enrichment analysis (GSEA) revealed that elevated SPOP expression correlated with downregulation of the Wnt signaling pathway **(Figure 3b)**. Using the STRING database, protein–protein interaction (PPI) analysis indicated that SPOP physically interacts with β-catenin, the product of the CTNNB1 gene **(Figure 3c)**. This interaction was further validated by immunoprecipitation coupled with mass spectrometry (IP–MS), which identified β-catenin as a binding partner of SPOP, with the specific binding peptides **(Figure 3d)**.

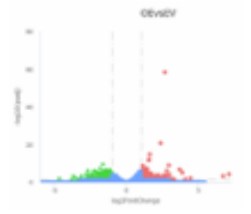

a)

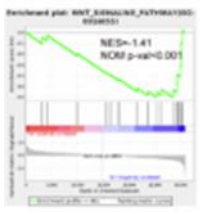

b)

c)

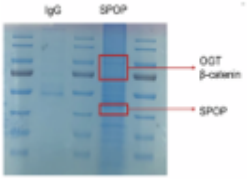

d)

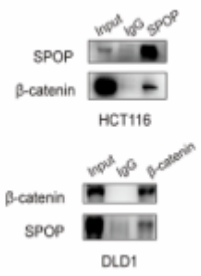

e)

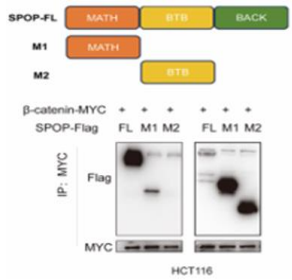

g)

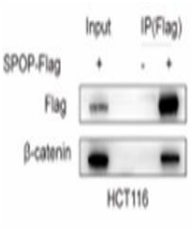

f)

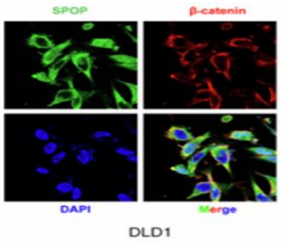

h)

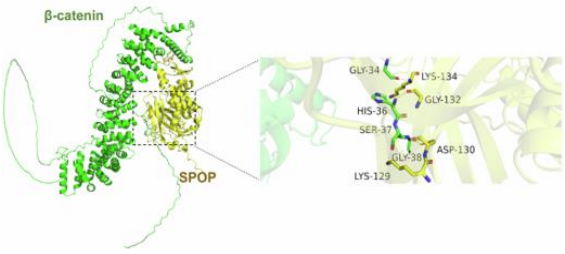

i)

Figure 3. Interaction between SPOP and β-Catenin **a** Transcriptome profiling via RNA-seq was conducted in HCT116 cells overexpressing SPOP. **b** Gene set enrichment analysis (GSEA) of RNA-seq data revealed that overexpression of SPOP led to suppression of Wnt signaling activity. **c** STRING database analysis illustrated the protein–protein interaction network of SPOP with Wnt pathway components. **d** Coomassie blue staining following anti-SPOP immunoprecipitation in HCT116 cells; the captured SPOP complexes were subsequently analyzed by mass spectrometry. **e, f** Co-immunoprecipitation (Co-IP) experiments confirmed interactions between both endogenous and exogenous SPOP and β-catenin. **g** Diagram depicting full-length and truncated SPOP mutants; Co-IP experiments showed the requirement of specific domains for β-catenin binding in HCT116 cells. **h** Immunofluorescence analysis in DLD-1 cells confirmed colocalization of SPOP and β-catenin; scale bars, 20 μm. **i** Molecular docking model

identifying interaction interfaces between SPOP and β-catenin.

Co-IP experiments verified that SPOP physically associates with β-catenin in both endogenous and exogenous contexts **(Figures 3e and 3f)**. The MATH domain of SPOP is essential for its E3 ligase function, mediating substrate recognition and binding. To investigate whether β-catenin binding depends on the MATH domain, we generated truncated SPOP mutants lacking either the MATH domain (M1) or the BTB domain (M2). Co-IP assays demonstrated that mutants retaining the MATH domain were capable of binding β-catenin, whereas BTB-only mutants could not **(Figure 3g)**, indicating that β-catenin recognition by SPOP requires the MATH domain.

Immunofluorescence further confirmed the colocalization of SPOP with β-catenin in CRC cells **(Figure 3h)**. Molecular docking predicted that Lys129, Asp130, Gly132, and Lys134 within SPOP are key residues for β-catenin binding **(Figure 3i)**. The G132V mutation of SPOP, previously reported as a pathogenic variant that elevates BRD4 levels [24], was introduced into SPOP, and Co-IP results showed that this mutation reduced β-catenin binding, confirming Gly132 as a critical residue for the interaction.

SPOP modulates β-catenin protein levels

In CRC cells, altering SPOP expression did not affect β-catenin mRNA levels **(Figure 4a)**. However, SPOP depletion resulted in increased β-catenin protein, while overexpression of SPOP reduced its protein abundance **(Figure 4b)**, suggesting that SPOP regulates β-catenin through a posttranslational mechanism rather than transcriptional control.

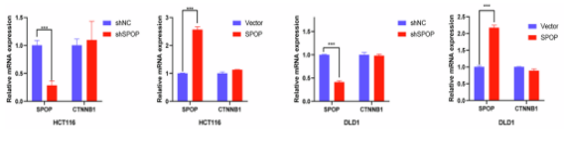

a)

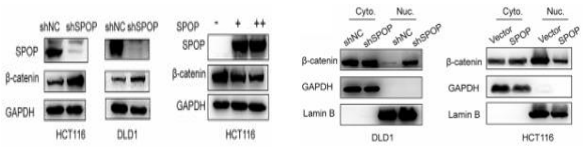

b) c)

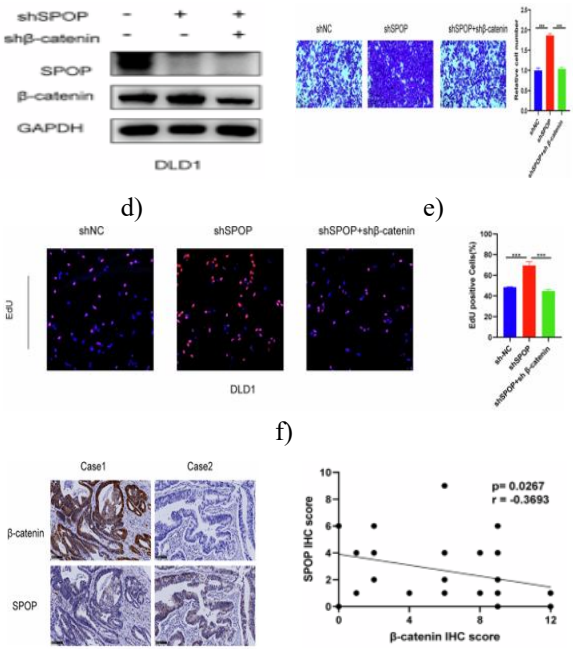

d) e) f)

g) h)

Figure 4. SPOP Controls β-Catenin Protein Levels Without Altering Its Transcription

a Quantitative RT–PCR showed that manipulating SPOP expression in HCT116 and DLD1 cells did not change β-catenin mRNA levels. **b** Western blotting revealed that reducing SPOP increased β-catenin protein, while overexpressing SPOP lowered its abundance. **c** Fractionation experiments demonstrated that nuclear β-catenin accumulation rose when SPOP was silenced and decreased under SPOP overexpression. **d** Co-silencing SPOP and β-catenin in DLD1 cells allowed assessment of their combined impact on protein expression. **e** Transwell assays showed that β-catenin knockdown counteracted the enhanced migration induced by SPOP depletion. **f** EdU proliferation assays indicated that β-catenin co-silencing reduced the proliferative effect of SPOP knockdown. **g** Representative IHC images of SPOP and β-catenin in 36 CRC patient samples; scale bars, 100 μm. **h** Spearman correlation based on H-score analysis demonstrated an inverse relationship between SPOP and β-catenin in tumor tissues.

Since nuclear β-catenin interacts with TCF4 to drive expression of genes promoting tumor progression [25, 26], we examined its localization and observed increased nuclear accumulation upon SPOP depletion, whereas SPOP overexpression reduced nuclear β-catenin **(Figure**

4c). To further test their functional interplay, CRC cells were co-transfected with shRNAs targeting both SPOP and β-catenin. Dual knockdown alleviated the pro-migratory and pro-proliferative effects caused by SPOP silencing, as shown by transwell and EdU assays **(Figures 4e and 4f)**. IHC analysis confirmed a strong negative correlation between SPOP and β-catenin expression in CRC tissues, consistent with the in vitro findings **(Figures 4g and 4h)**.

SPOP enhances β-catenin ubiquitination

Given SPOP's role as an E3 ubiquitin ligase, we hypothesized that it regulates β-catenin stability through the ubiquitin–proteasome system. Overexpression of SPOP in HCT116 and DLD1 cells followed by treatment with the proteasome inhibitor MG132 restored β-catenin levels, indicating proteasomal involvement **(Figure 5a)**. Cycloheximide chase experiments showed that silencing SPOP prolonged β-catenin half-life, confirming that SPOP accelerates its turnover **(Figure 5b)**. Ubiquitination assays further demonstrated that SPOP knockdown reduced, whereas SPOP overexpression enhanced, β-catenin ubiquitination **(Figures 5c and 5d)**. The G132V mutant of SPOP, known for impaired substrate binding, failed to promote β-catenin ubiquitination, highlighting the functional importance of this residue.

Considering that the MATH domain of SPOP recognizes the SPOP-binding consensus (SBC) motif in substrates [27], we identified two potential SBC motifs in β-catenin and generated truncation mutants (SBC1 and SBC2) **(Figure 5e)**. Co-immunoprecipitation revealed that the SBC2 mutant lost interaction with SPOP **(Figure 5f)** and displayed substantially reduced ubiquitination levels **(Figure 5g)**, demonstrating that the SBC2 site is critical for SPOP-mediated β-catenin regulation.

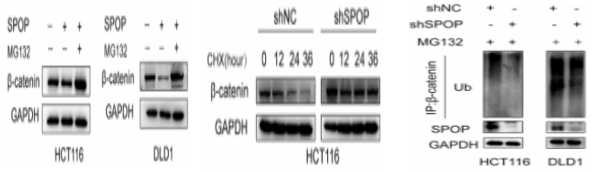

a) b) c)

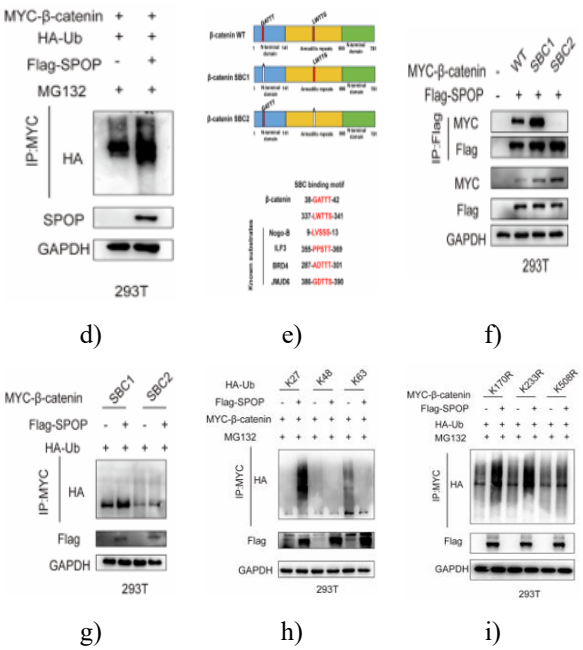

d) e) f)

g) h) i)

Figure 5. SPOP Facilitates β-Catenin Ubiquitination and Proteasomal Degradation

a Western blot analysis of β-catenin in HCT116 and DLD1 cells overexpressing SPOP after treatment with the proteasome inhibitor MG132 (10 μM, 6 h). **b** HCT116 cells transfected with shSPOP were treated with cycloheximide (CHX) and collected at multiple time points to assess β-catenin stability via western blot. **c** Total β-catenin ubiquitination in SPOP-knockdown HCT116 and DLD1 cells transfected with appropriate plasmids (48 h) and treated with MG132 (10 μM, 6 h). **d** 293T cells were co-transfected with MYC-β-catenin, HA-Ub, and Flag-SPOP, and ubiquitination was assessed by IP. **e** Sequence alignment of β-catenin with SBC motifs found in known SPOP substrates. **f** IP analysis of 293T cells transfected with MYC-β-catenin-SBC1 or SBC2 mutants together with Flag-SPOP. **g** Ubiquitination assays of β-catenin SBC mutants in 293T cells co-expressing HA-Ub and Flag-SPOP. **h** Assessment of β-catenin ubiquitination in 293T cells co-expressing MYC-β-catenin, HA-Ub linkage mutants (K27, K48, K63), and Flag-SPOP. **i** IP-based ubiquitination analysis of K-to-R β-catenin mutants (K170R, K233R, K508R) in 293T cells co-expressing HA-Ub and Flag-SPOP.

Previous studies reported that β-catenin can be modified via K27-, K48-, and K63-linked polyubiquitination [28]. Our experiments showed that SPOP overexpression

specifically enhanced K27-linked β-catenin ubiquitination, without affecting K48- or K63-linked chains **(Figure 5h)**. To pinpoint the lysine residue targeted by SPOP, the PhosphoSitePlus® database was used to identify potential ubiquitination sites on β-catenin, selecting K170, K233, and K508 for mutagenesis. Ubiquitination assays revealed that only the K508R mutation blocked SPOP-mediated β-catenin ubiquitination **(Figure 5i)**, indicating that K508 is the critical site for SPOP-dependent ubiquitination.

O-GlcNAcylation modulates SPOP–β-catenin interaction

IP-MS data identified OGT as a potential SPOP-interacting protein. Consistent with prior reports in PDAC and 293T cells [29], Co-IP experiments confirmed that SPOP interacts with OGT in CRC cell lines as well **(Figure 6a)**. Overexpression of OGT led to increased O-GlcNAc modification levels but decreased SPOP protein abundance **(Figure 6b)**, whereas OGT knockdown produced the opposite effect **(Figure 6c)**.

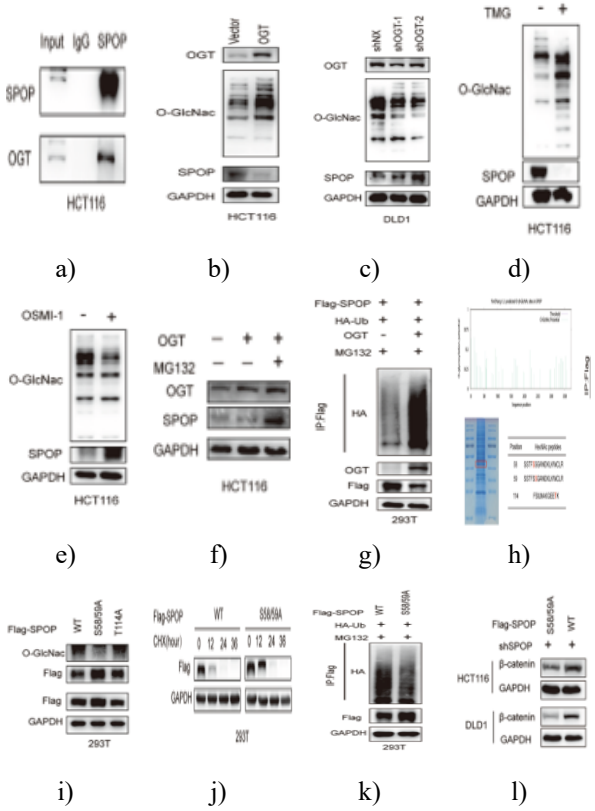

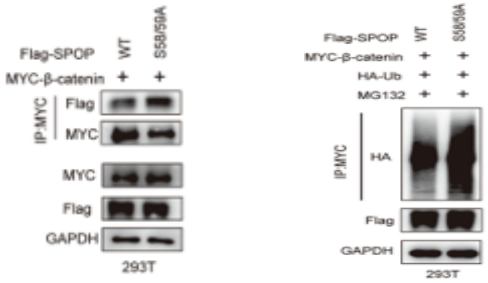

Figure 6. O-GlcNAcylation of SPOP Modulates Its Binding to β-Catenin

a Co-IP experiments confirmed interaction between endogenous SPOP and OGT. **b** Western blot analysis of SPOP levels in HCT116 cells following OGT overexpression. **c** SPOP expression in DLD1 cells after shOGT-mediated knockdown. **d, e** Western blot showing SPOP protein levels in HCT116 cells treated with the OGA inhibitor TMG or the OGT inhibitor OSMI-1, respectively. **f** SPOP expression in OGT-overexpressing HCT116 cells treated with MG132 (10 μM, 6 h). **g** IP analysis of SPOP ubiquitination in 293T cells co-transfected with HA-Ub, OGT, and Flag-SPOP. **h** MS identification of potential O-GlcNAcylation sites on SPOP. **i** IP assays examining O-GlcNAc levels in SPOP point mutants (S58/S59A, T114A). j CHX chase assay assessing the stability of SPOP-S58/S59A versus wild-type SPOP in 293T cells. k Ubiquitination analysis of SPOP mutants compared to SPOP-WT. l, m WB and IP assays evaluating β-catenin protein levels and binding to SPOP-S58/S59A versus SPOP-WT. n Ubiquitination of β-catenin in 293T cells co-expressing HA-Ub, MYC-β-catenin, and either SPOP-WT or S58/S59A mutant.

Treatment with the OGT inhibitor OSMI-1 increased SPOP protein abundance, whereas TMG treatment, which elevates O-GlcNAc levels, reduced SPOP expression in HCT116 cells **(Figures 6d and 6e)**, indicating that O-GlcNAcylation negatively regulates SPOP levels. To determine whether this regulation occurs via the ubiquitin–proteasome system, OGT-overexpressing HCT116 cells were treated with MG132. Proteasome inhibition prevented OGT-induced SPOP degradation **(Figure 6f)**, and IP assays revealed increased ubiquitination of SPOP upon OGT overexpression **(Figure 6g)**, suggesting that O-GlcNAcylation promotes proteasome-mediated SPOP degradation.

Mass spectrometry identified three potential O-GlcNAcylation sites on SPOP (S58, S59, T114) **(Figure 6h)**. Point mutants S58/S59A and T114A were generated, and IP experiments showed that S58/S59A markedly reduced O-GlcNAc modification **(Figure 6i)**, designating these residues as major glycosylation sites. The S58/S59A mutant exhibited accelerated degradation **(Figure 6j)** and increased ubiquitination compared with SPOP-WT **(Figure 6k)**.

We further examined how O-GlcNAcylation affects SPOP's interaction with β-catenin. The S58/S59A mutant demonstrated enhanced binding to β-catenin and reduced β-catenin protein levels compared with SPOP-WT **(Figures 6l and 6m)**, accompanied by increased β-catenin ubiquitination **(Figure 6n)**. These findings indicate that O-GlcNAcylation of SPOP impairs its ability to bind β-catenin, thereby stabilizing β-catenin and preventing its degradation.

SPOP promotes ferroptosis in CRC

To explore the role of SPOP in CRC growth regulation, KEGG pathway analysis using TCGA data highlighted ferroptosis among the top enriched pathways **(Figure 7a)**. Functional assays revealed that SPOP overexpression enhanced the growth-inhibitory effects of the ferroptosis inducer erastin in CRC cells. This effect was specifically reversed by the ferroptosis inhibitor Ferrostatin-1 (Fer-1), whereas inhibitors of other forms of regulated cell death, such as necroptosis (Nec-1) and apoptosis (Z-VAD-FMK), had no impact **(Figure 7b)**.

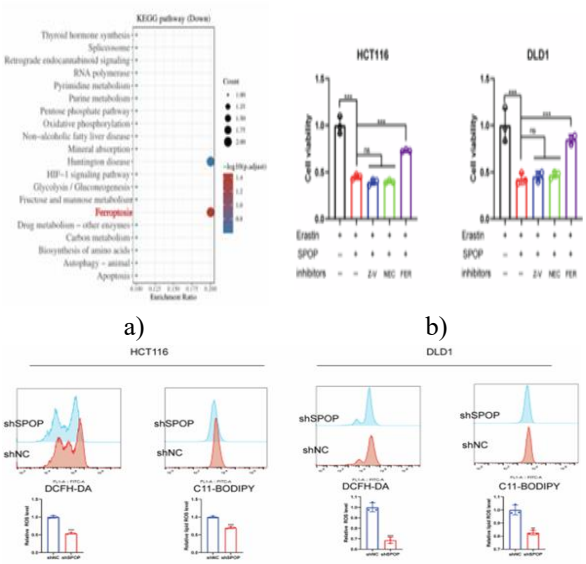

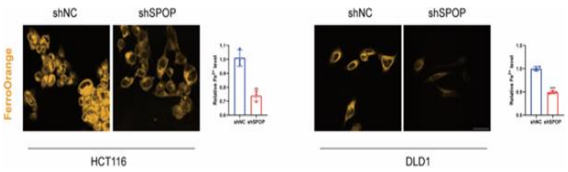

Figure 7. SPOP enhances ferroptosis in colorectal cancer cells

a KEGG pathway enrichment analysis highlighting the top 10 pathways in CRC. **b** CRC cells were transfected with an SPOP overexpression plasmid for 24 h, seeded at 5000 cells per well in 96-well plates, and treated with 10 μM erastin alone or combined with 2 μM Fer-1, 10 μM Z-VAD-FMK, or 5 μM Nec-1 for 48 h. **c** CRC cells with shSPOP knockdown were exposed to 10 μM erastin for 24 h and stained with DCFH-DA and C11-BODIPY to assess ROS and lipid peroxidation via flow cytometry. **d** Intracellular Fe^{2+} levels in SPOP-knockdown CRC cells were detected using FerroOrange; scale bars, 20 μm.

Analysis of ROS and lipid peroxidation using DCFH-DA and C11-BODIPY probes revealed that SPOP knockdown markedly reduced both ROS and lipid ROS levels in CRC cells **(Figure 7c)**. Similarly, measurements of Fe^{2+} with FerroOrange showed a significant decline in intracellular iron following SPOP depletion **(Figure 7d)**, indicating that SPOP enhances CRC cell susceptibility to ferroptosis.

SPOP modulates ferroptosis via the β-Catenin/SLC7A11 pathway

To clarify how SPOP regulates ferroptosis, we examined the ChIP-Atlas database, which revealed a β-catenin/TCF4 binding peak at the SLC7A11 promoter in HCT116 cells **(Figure 8a)**. qPCR analysis demonstrated that SPOP overexpression decreased SLC7A11 mRNA levels **(Figure 8b)**, implying transcriptional regulation. Given that SPOP interacts with β-catenin, we hypothesized that SPOP controls SLC7A11 expression through β-catenin **(Figure 8c)**.

Consistent with this, β-catenin overexpression upregulated SLC7A11 mRNA, and dual-luciferase reporter assays confirmed that β-catenin enhances SLC7A11 promoter activity, whereas co-expression of SPOP attenuated this effect **(Figure 8f)**. Notably, the β-catenin K508R mutant further increased SLC7A11 promoter activity compared with wild-type β-catenin

(Figure 8g), indicating that SPOP regulates the transcriptional function of β-catenin on SLC7A11. JASPAR predictions identified β-catenin/TCF4 binding motifs within the SLC7A11 promoter **(Figure 8h)**, and ChIP-qPCR experiments verified this interaction **(Figures 8i and 8j)**, aligning with database predictions. Overexpression of SPOP decreased the protein levels of both β-catenin and SLC7A11 **(Figure 8k)**, supporting the concept that the SPOP/β-catenin/SLC7A11 axis plays a critical role in modulating ferroptosis in CRC cells.

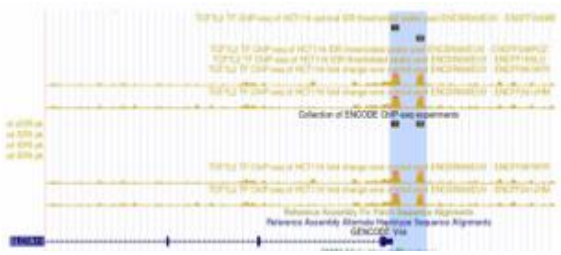

a)

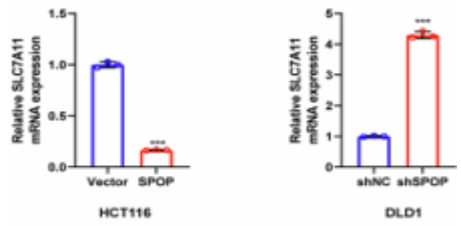

b)

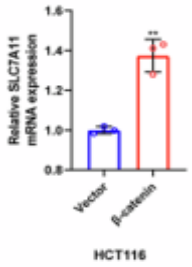

c)

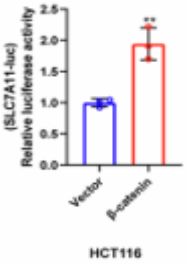

d)

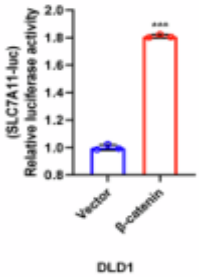

e)

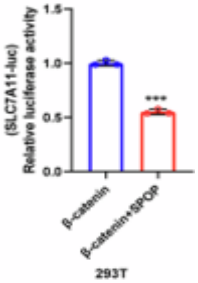

f)

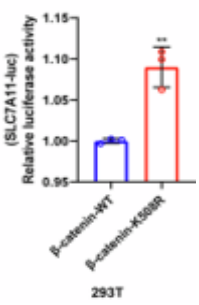

g)

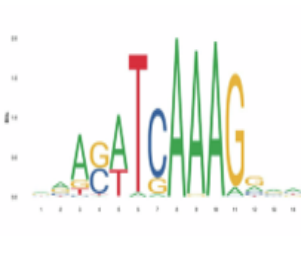

h)

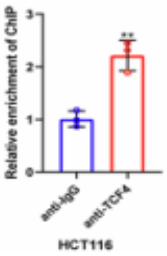

i)

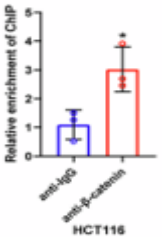

j)

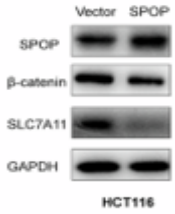

k)

Figure 8. Regulation of Ferroptosis in CRC via the SPOP/β-Catenin/SLC7A11 Axis

a ChIP-seq analysis showing TCF4 binding within the SLC7A11 promoter region. **b** qRT-PCR detection of SLC7A11 mRNA in DLD1 cells after shSPOP knockdown and in HCT116 cells following SPOP overexpression. **c** Measurement of SLC7A11 mRNA levels in HCT116 cells transfected with a β-catenin overexpression plasmid. **d–g** Dual-luciferase reporter assays assessing SLC7A11 promoter activity under various conditions. **h** Predicted TCF4-binding motif within the SLC7A11 promoter from the JASPAR database. **i, j** ChIP-qPCR verification of TCF4 and β-catenin occupancy at the SLC7A11 promoter. K Western blot analysis of HCT116 cells transfected with SPOP-overexpressing plasmids.

Synergistic antitumor activity of maprotiline and ferroptosis inducers

Maprotiline (MAP) directly binds to SPOP, enhancing its activity and regulating PD-L1 ubiquitination, thereby

exerting anticancer effects and increasing SPOP protein levels. In CRC cell lines, MAP treatment reduced both proliferation and migration and elevated β-catenin ubiquitination. Additionally, MAP increased intracellular lipid ROS in a dose-dependent manner, indicating its potential to promote ferroptosis.

To evaluate whether MAP could sensitize CRC cells to ferroptosis, we combined MAP with the ferroptosis inducer erastin. The combination treatment significantly inhibited CRC cell growth compared with either agent alone **(Figure 9a)**, and the combination index (CI) was below 1 **(Figure 9b)**, indicating synergism [30]. Flow cytometry further confirmed that lipid ROS levels were markedly higher in the combination group relative to erastin alone **(Figure 9c)**, supporting enhanced ferroptotic activity.

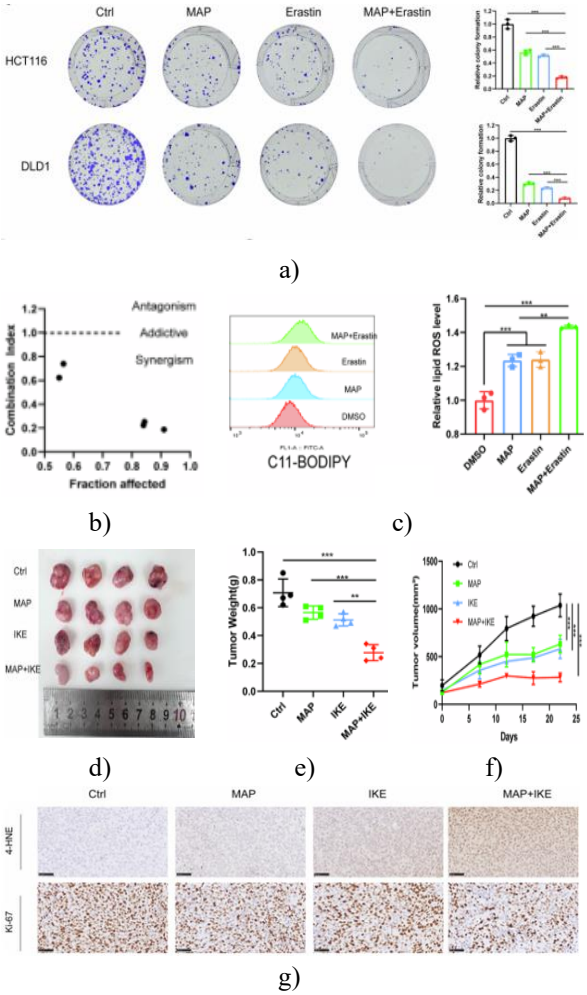

Figure 9. Synergistic antitumor effects of MAP and ferroptosis inducers in CRC

a Colony formation assays assessing CRC cell growth under different concentrations of MAP, ferroptosis inducers, and their combination. **b** Calculation of the combination index (CI) for MAP and erastin in HCT116 cells using CalcuSyn software. **c** Lipid ROS levels were detected via C11-BODIPY staining. **d** Representative images of subcutaneous xenograft tumors (n = 4). **e** Quantification of tumor weights. **f** Tumor growth curves over time. g Immunohistochemical staining of xenografts for 4-HNE and Ki67; scale bars, 50 μm.

To evaluate the in vivo efficacy of the combination, HCT116 xenografts were established, and after one week, mice received daily oral MAP (30 mg/kg) and intraperitoneal IKE (40 mg/kg) every 2 days for 3 weeks. Tumors in the combination treatment group exhibited markedly reduced volume and weight and slower growth compared with the IKE-only group **(Figures 9d–9f)**. Immunohistochemistry further demonstrated elevated 4-HNE levels, a ferroptosis marker, and reduced Ki67 staining, consistent with enhanced ferroptotic activity **(Figure 9g)**.

Biosafety evaluation showed no significant changes in body weight among treatment groups, and histopathology of major organs revealed no notable morphological alterations. Collectively, these results suggest that MAP, alone or in combination with IKE, exhibits potent anticancer effects while maintaining a favorable safety profile.

Our study demonstrates that SPOP functions as a tumor suppressor in CRC. SPOP expression is downregulated in CRC tissues, correlates with improved patient survival, and inversely associates with β-catenin protein levels. Functionally, SPOP suppresses proliferation and metastasis while enhancing CRC sensitivity to ferroptosis. Mechanistically, SPOP directly interacts with β-catenin, promoting ubiquitination and degradation at the K508 residue, thereby inhibiting downstream SLC7A11 activation. Moreover, O-GlcNAcylation of SPOP modulates its stability and activity, affecting this regulatory pathway. Clinically, MAP, a SPOP-targeting drug, synergizes with the ferroptosis inducer IKE to inhibit CRC growth.

Posttranslational modifications such as ubiquitination are crucial for protein regulation, and dysregulation of the ubiquitin–proteasome system is implicated in cancer development and metastasis [16]. Thus, targeting E3 ubiquitin ligases and their substrates, including through approaches like PROTACs, is a major focus in current oncology research. Ferroptosis represents a promising

strategy for drug-resistant CRC, and our study identifies a novel regulatory mechanism linking PTMs with ferroptosis sensitivity.

We show that SPOP-mediated β-catenin degradation is critical in CRC. β-Catenin, a central Wnt pathway component [31], influences tumor progression and ferroptosis. Previous studies indicate that β-catenin/TCF4 enhances GPX4 expression to inhibit ferroptosis in gastric cancer [32] and that MsrB/β-catenin suppresses ferroptosis in CRC [33]. In prostate cancer, SPOP promotes ferroptosis by degrading JMJD6, affecting ATF4-mediated SLC7A11 expression [34]. In contrast, our data reveal that SPOP induces β-catenin polyubiquitination, reduces its stability, diminishes its promoter binding at SLC7A11, and promotes ferroptosis in CRC.

These findings underscore the multifaceted role of SPOP as an E3 ligase in regulating target protein degradation and ferroptosis. Interestingly, SPOP has been reported to enhance β-catenin/TCF4 activity in clear cell renal cell carcinoma [35], whereas in CRC, it suppresses tumor progression via β-catenin degradation, likely reflecting tumor-type heterogeneity. To our knowledge, this is the first report demonstrating that SPOP binds β-catenin, increases its ubiquitination, and drives its degradation, revealing a previously uncharacterized mechanism in CRC.

O-GlcNAcylation, a posttranslational modification targeting serine or threonine residues, occurs on intracellular proteins and is dynamically regulated by OGT and OGA [36]. This modification has been implicated in cancer therapy resistance and exhibits crosstalk with ubiquitination [37]. Ubiquitination can influence protein stability and subcellular localization, which may indirectly affect the O-GlcNAcylation of ENO1 at Ser249, potentially disrupting its interaction with PD-L1 and reducing PD-L1 recognition by the E3 ligase STUB1, thereby stabilizing PD-L1 and promoting CRC progression [38]. In our study, we demonstrated that SPOP interacts with OGT, which in turn regulates SPOP ubiquitination and protein stability. LC–MS analysis identified O-GlcNAcylation sites at S58 and S59 of SPOP in CRC, and this modification modulates SPOP binding to β-catenin and alters β-catenin ubiquitination, highlighting the critical role of O-GlcNAcylation in controlling SPOP function in CRC.

Previous research has shown that combining MAP with anti-CTLA4 therapy enhances antitumor efficacy in CRC and lung cancer patients by targeting SPOP at Arg70, increasing SPOP protein levels, and promoting PD-L1 ubiquitination. In hepatocellular carcinoma, MAP combined with the ferroptosis inducer sorafenib markedly potentiated tumor inhibition [39], indicating that MAP sensitizes cells to ferroptosis. Our results further show that MAP regulates β-catenin ubiquitination, suppressing CRC cell proliferation and migration while increasing lipid peroxidation, thereby contributing to its anticancer effects. In vivo, the combination of MAP and IKE produced synergistic tumor inhibition with a favorable safety profile.

Despite these findings, the specific E3 ligases responsible for SPOP ubiquitination remain to be identified. Moreover, although the MAP and IKE combination effectively suppressed CRC growth, validation in clinically relevant organoid and patient-derived xenograft (PDX) models is needed to confirm its translational potential.

Materials and Methods

Cell culture

Human colorectal cancer (CRC) cell lines HCT116 and DLD1, along with 293T cells, were obtained from the Stem Cell Bank of the Chinese Academy of Sciences. Upon receipt, cells were maintained in DMEM (Gibco) supplemented with 10% fetal bovine serum (FBS; Gibco, 10099) and incubated at 37 °C under a humidified atmosphere containing 5% CO_2.

Mass spectrometry (MS) analysis

To identify novel SPOP-interacting proteins, HCT116 cells were transfected with Flag-tagged SPOP plasmids. SPOP protein complexes were immunoprecipitated at 4 °C using an anti-SPOP antibody and protein A/G beads (HY-K0202). Subsequent LC–MS/MS analysis was conducted by Cosmos Wisdom Biotech Co., Ltd. (Hangzhou, China). Mass spectra were processed and matched against the human Swissprot database (release 2023_09) using Proteome Discoverer (v2.4, Thermo Scientific).

Animal experiments

All animal studies were approved by the Ethics Committee of the Second Affiliated Hospital of Zhejiang University School of Medicine (Approval No. 2024-120). Female BALB/c nude mice (4–5 weeks old) were purchased from Shanghai BK Laboratory Animal Co., Ltd. HCT116 cells were harvested, mixed 1:1 with

Matrigel, and 4 × 10^6 cells in 100 µL were injected subcutaneously into each mouse. Once tumor volumes reached approximately 100 mm^3, mice were randomized into four treatment groups. Tumor volumes were calculated using the formula: volume (mm^3) = L × S × S / 2.

Statistical analysis

All quantitative analyses were conducted using GraphPad Prism 8 (San Diego, CA, USA). Data are presented as mean ± standard deviation (SD). Comparisons between two groups were performed using unpaired t-tests, while multiple-group comparisons employed one-way ANOVA followed by Tukey's post hoc test. Spearman's correlation coefficient was used for correlation analyses. A p-value < 0.05 was considered statistically significant.

Acknowledgments: None

Conflict of Interest: None

Financial Support: None

Ethics Statement: None

References

1. Bray F, Laversanne M, Sung H, Ferlay J, Siegel RL, Soerjomataram I, et al. Global cancer statistics 2022: GLOBOCAN estimates of incidence and mortality worldwide for 36 cancers in 185 countries. CA Cancer J Clin. 2024;74:229–63
2. Di Nicolantonio F, Vitiello PP, Marsoni S, Siena S, Tabernero J, Trusolino L, et al. Precision oncology in metastatic colorectal cancer - from biology to medicine. Nat Rev Clin Oncol. 2021;18:506–25.
3. Biller LH, Schrag D. Diagnosis and Treatment of Metastatic Colorectal Cancer: A Review. JAMA. 2021;325:669–85.
4. Morin PJ, Sparks AB, Korinek V, Barker N, Clevers H, Vogelstein B, et al. Activation of beta-catenin-Tcf signaling in colon cancer by mutations in beta-catenin or APC. Science. 1997;275:1787–90.
5. Petroski MD, Deshaies RJ. Function and regulation of cullin-RING ubiquitin ligases. Nat Rev Mol Cell Biol. 2005;6:9–20.
6. Song Y, Xu Y, Pan C, Yan L, Wang ZW, Zhu X. The emerging role of SPOP protein in tumorigenesis and cancer therapy. Mol Cancer. 2020;19:2.
7. Cheng J, Guo J, Wang Z, North BJ, Tao K, Dai X, et al. Functional analysis of Cullin 3 E3 ligases in tumorigenesis. Biochim Biophys Acta Rev Cancer. 2018;1869:11–28.
8. Chen RH. Cullin 3 and Its Role in Tumorigenesis. Adv Exp Med Biol. 2020;1217:187–210.
9. Zhou Q, Lin W, Wang C, Sun F, Ju S, Chen Q, et al. Neddylation inhibition induces glutamine uptake and metabolism by targeting CRL3(SPOP) E3 ligase in cancer cells. Nat Commun. 2022;13:3034.
10. Zeng C, Wang Y, Lu Q, Chen J, Zhang J, Liu T, et al. SPOP suppresses tumorigenesis by regulating Hedgehog/Gli2 signaling pathway in gastric cancer. J Exp Clin Cancer Res. 2014;33:75.
11. Geng C, Rajapakshe K, Shah SS, Shou J, Eedunuri VK, Foley C, et al. Androgen receptor is the key transcriptional mediator of the tumor suppressor SPOP in prostate cancer. Cancer Res. 2014;74:5631–43.
12. Jin X, Wang J, Li Q, Zhuang H, Yang J, Lin Z, et al. SPOP targets oncogenic protein ZBTB3 for destruction to suppress endometrial cancer. Am J Cancer Res. 2019;9:2797–812.
13. Jin X, Shi Q, Li Q, Zhou L, Wang J, Jiang L, et al. CRL3-SPOP ubiquitin ligase complex suppresses the growth of diffuse large B-cell lymphoma by negatively regulating the MyD88/NF-kappaB signaling. Leukemia. 2020;34:1305–14.
14. Yao S, Chen X, Chen J, Guan Y, Liu Y, Chen J, et al. Speckle-type POZ protein functions as a tumor suppressor in non-small cell lung cancer due to DNA methylation. Cancer Cell Int. 2018;18:213.
15. Li M, Cui Y, Qi Q, Liu J, Li J, Huang G, et al. SPOP downregulation promotes bladder cancer progression based on cancer cell-macrophage crosstalk via STAT3/CCL2/IL-6 axis and is regulated by VEZF1. Theranostics. 2024;14:6543–59.
16. Zhang H, Jin X, Huang H. Deregulation of SPOP in Cancer. Cancer Res. 2023;83:489–99.
17. Dixon SJ, Lemberg KM, Lamprecht MR, Skouta R, Zaitsev EM, Gleason CE, et al. Ferroptosis: an iron-dependent form of nonapoptotic cell death. Cell. 2012;149:1060–72.

18. Zhao L, Zhou X, Xie F, Zhang L, Yan H, Huang J, et al. Ferroptosis in cancer and cancer immunotherapy. Cancer Commun. 2022;42:88–116.
19. Lei S, Chen C, Han F, Deng J, Huang D, Qian L, et al. AMER1 deficiency promotes the distant metastasis of colorectal cancer by inhibiting SLC7A11- and FTL-mediated ferroptosis. Cell Rep. 2023;42:113110.
20. Koppula P, Zhuang L, Gan B. Cystine transporter SLC7A11/xCT in cancer: ferroptosis, nutrient dependency, and cancer therapy. Protein Cell. 2021;12:599–620. Article PubMed CAS Google Scholar
21. Wang L, Liu Y, Du T, Yang H, Lei L, Guo M, et al. ATF3 promotes erastin-induced ferroptosis by suppressing system Xc. Cell Death Differ. 2020;27:662–75.
22. Tang B, Zhu J, Liu F, Ding J, Wang Y, Fang S, et al. xCT contributes to colorectal cancer tumorigenesis through upregulation of the MELK oncogene and activation of the AKT/mTOR cascade. Cell Death Dis. 2022;13:373.
23. Tang J, Long G, Xiao D, Liu S, Xiao L, Zhou L, et al. ATR-dependent ubiquitin-specific protease 20 phosphorylation confers oxaliplatin and ferroptosis resistance. MedComm. 2023;4:e463 (2020).
24. Nabais Sa MJ, El Tekle G, de Brouwer APM, Sawyer SL, Del Gaudio D, Parker MJ, et al. De Novo Variants in SPOP Cause Two Clinically Distinct Neurodevelopmental Disorders. Am J Hum Genet. 2020;106:405–11.
25. MacDonald BT, Tamai K, He X. Wnt/beta-catenin signaling: components, mechanisms, and diseases. Dev Cell. 2009;17:9–26.
26. Zhu Y, Gu L, Lin X, Cui K, Liu C, Lu B, et al. LINC00265 promotes colorectal tumorigenesis via ZMIZ2 and USP7-mediated stabilization of beta-catenin. Cell Death Differ. 2020;27:1316–27.
27. Zhuang M, Calabrese MF, Liu J, Waddell MB, Nourse A, Hammel M, et al. Structures of SPOP-substrate complexes: insights into molecular architectures of BTB-Cul3 ubiquitin ligases. Mol Cell. 2009;36:39–50.
28. Guo Y, Tian J, Guo Y, Wang C, Chen C, Cai S, et al. Oncogenic KRAS effector USP13 promotes metastasis in non-small cell lung cancer through deubiquitinating beta-catenin. Cell Rep. 2023;42:113511.
29. Zhou P, Chang WY, Gong DA, Huang LY, Liu R, Liu Y, et al. O-GlcNAcylation of SPOP promotes carcinogenesis in hepatocellular carcinoma. Oncogene. 2023;42:725–36
30. Jin X, Lv Y, Bie F, Duan J, Ma C, Dai M, et al. METTL3 confers oxaliplatin resistance through the activation of G6PD-enhanced pentose phosphate pathway in hepatocellular carcinoma. Cell Death Differ. 2025;32:466–79.
31. Tufail M, Jiang CH, Li N. Wnt signaling in cancer: from biomarkers to targeted therapies and clinical translation. Mol Cancer. 2025;24:107.
32. Wang Y, Zheng L, Shang W, Yang Z, Li T, Liu F, et al. Wnt/beta-catenin signaling confers ferroptosis resistance by targeting GPX4 in gastric cancer. Cell Death Differ. 2022;29:2190–202.
33. Gao Z, Yang S, Jiang S, Wu Q, Jia Y, Zhang M, et al. Transcription factor KLF5 regulates MsrB1 to promote colorectal cancer progression by inhibiting ferroptosis through beta-catenin. Free Radic Biol Med. 2025;234:34–48.
34. Zhang C, Ding J, Lim KS, Zhou W, Miao W, Wu S, et al. JMJD6 Rewires ATF4-Dependent Glutathione Metabolism to Confer Ferroptosis Resistance in SPOP-Mutated Prostate Cancer. Cancer Res. 2025;85:1496–513.
35. Zhao W, Zhou J, Deng Z, Gao Y, Cheng Y. SPOP promotes tumor progression via activation of beta-catenin/TCF4 complex in clear cell renal cell carcinoma. Int J Oncol. 2016;49:1001–8.
36. He XF, Hu X, Wen GJ, Wang Z, Lin WJ. O-GlcNAcylation in cancer development and immunotherapy. Cancer Lett. 2023;566:216258.
37. Sun K, Zhi Y, Ren W, Li S, Zheng J, Gao L, et al. Crosstalk between O-GlcNAcylation and ubiquitination: a novel strategy for overcoming cancer therapeutic resistance. Exp Hematol Oncol. 2024;13:107.
38. Zhu Q, Li J, Sun H, Fan Z, Hu J, Chai S, et al. O-GlcNAcylation of enolase 1 serves as a dual regulator of aerobic glycolysis and immune evasion in colorectal cancer. Proc Natl Acad Sci USA. 2024;121:e2408354121.
39. Zheng C, Zhu Y, Liu Q, Luo T, Xu W. Maprotiline Suppresses Cholesterol Biosynthesis and Hepatocellular Carcinoma Progression Through Direct Targeting of CRABP1. Front Pharm. 2021;12:689767.